

The Stress c-Jun N-terminal Kinase Signaling Pathway Activation Correlates with Synaptic Pathology and Presents A Sex Bias in P301L Mouse Model of Tauopathy

Lucia Buccarello,^{a,b} Clara Alice Musi,^b Arianna Turati^b and Tiziana Borsello^{a,b,*}

^a Department of Pharmacological and Biomolecular Sciences, Milan University, Italy

^b Department of Neuroscience, Mario Negri Institute for Pharmacological Research-IRCCS, Milan, Italy

Abstract—Pathological Tau (P-Tau) leads to dementia and neurodegeneration in tauopathies, including Alzheimer's disease. The P301L transgenic mice well mimic human tauopathy features; P-Tau localizes also at the dendritic spine level and this correlates with synaptic markers down-regulation. Importantly, tg female present a more severe pathology compared to male mice. We describe JNK activation in P301L-tg mice, characterizing by P-JNK and P-c-Jun, cleaved-Caspase-3, P-PSD95 and P-Tau (direct JNK-targets) increased levels in tg vs control mice. These data indicate that JNK stress pathway is involved in neuronal degenerative mechanisms of this mouse model. In addition, P-JNK level is higher in female compared to male tg mice, underlying a sexual dimorphism in the JNK pathway activation. The behavioral studies highlight that tg female present major cognitive and locomotor defects, strongly correlated with a more severe synaptic injury, in comparison to tg male. Notably, at the dendritic spine level, JNK is powerfully activated and its level reveals a sexual dimorphism that is coherent with behavioral defects and spine pathology. The P301L's synaptic pathology is characterized by a strong increase of P-PSD95/PSD95 and P-JNK/JNK ratios and by an augmented level of cleaved-Caspase-3 and a decrease of Drebrin level in the post-synaptic elements. These results suggest that JNK plays a key role in synaptopathy of P301L mice. Importantly, until now, there are any efficient treatments against synaptic pathology and JNK could represent an interesting target to tackle P-Tau-induced synaptic pathology. It will be important to test specific JNK inhibitors to verify their potential neuroprotective effect. © 2018 IBRO. Published by Elsevier Ltd. All rights reserved.

Keywords: synaptopathy, behavioral defects, synaptic dysfunction, Drebrin, cleaved-caspase-3, P-Tau protein.

INTRODUCTION

Tauopathies are a class of neurodegenerative diseases associated with the pathological aggregation of Tau protein in the human brain (Delacourte and Buée, 2000; Ingram and Spillantini, 2002; Yancopoulos and Spillantini, 2003; Yoshiyama et al., 2007). Tauopathies are characterized by abnormal accumulation of Tau protein in neurons, leading to cognitive and locomotor dysfunctions. Hyper-phosphorylated Tau (P-Tau) is a principal component of neurofibrillary tangles (NFTs),

which represent a typical hallmark of tauopathies. Major diseases with Tau pathology are: Alzheimer disease (AD), Pick disease (PD), corticobasal degeneration (CBD), progressive supranuclear palsy (PSP) (Yoshiyama et al., 2007), frontotemporal dementia with Parkinsonism linked to chromosome 17 (FTDP-17) (Yancopoulos and Spillantini, 2003). Recent studies underline the Tau role in neurodegeneration, such as in Alzheimer's disease (Hoover et al., 2010), is underestimated. In the tauopathies, Tau is hyper-phosphorylated and the pathological Tau (P-Tau) aggregates into neurofibrillary tangles at the somatic level in an age-dependent manner (Avila et al., 2004; Gendron and Petrucelli, 2009). In addition, P-Tau causes key morphological changes in neurons, such significant alterations in dendritic length and their complexities (Crimins et al., 2011, 2012; Rocher et al., 2010) as well as the reduction in dendritic spine number (Kopeikina et al., 2013; Thies and Mandelkow, 2007), impairs cellular trafficking (Roy et al., 2005; Shemesh et al., 2008; Thies and Mandelkow, 2007) and synaptic activity alteration (Hoover et al., 2010; Yoshiyama et al., 2007).

*Corresponding author. Address: Neuronal Death and Neuroprotection Lab, Department of Pharmacological and Biomolecular Sciences, CEND-Center of Excellence on Neurodegenerative Diseases, Università degli Studi di Milano, Via Balzaretti 9, 20133 Milano, Italy. Neuroscience Department, IRCCS-Istituto Di Ricerche Farmacologiche, "Mario Negri", Via la Masa 19, 20156 Milano, Italy. Fax: +39-0239001916.

E-mail addresses: tiziana.borsello@unimi.it, tiziana.borsello@mario-negri.it (T. Borsello).

Abbreviations: AD, Alzheimer's disease; APP, amyloid precursor protein; NFTs, neurofibrillary tangles; JNK, c-Jun N-terminal kinase; NORT, novel-object recognition test; OFT, open-field test; P-Tau, phospho-Tau.

<https://doi.org/10.1016/j.neuroscience.2018.09.049>

0306-4522/© 2018 IBRO. Published by Elsevier Ltd. All rights reserved.

In this contest, we examined P301L-tg's synaptopathy and its related intracellular pathways, focusing on the stress c-Jun N-terminal Kinase (JNK) that directly phosphorylates Tau (Ploia et al., 2011) and has a pivotal role in AD's synaptic injury (Scip et al., 2013, 2014). The synaptic dysfunction is the first neurodegenerative event and it is a core feature of many different brain disorders, underlying a common and initially reversible mechanism in these pathologies. Until now, no efficient treatment exists against synaptic pathology. Investigate the molecular mechanism of this crucial degenerative event is important to develop novel therapeutical strategies against many different neurological disorders. The P301L transgenic mouse model (JNPL3 mice) well mimic the feature of human tauopathies (Lewis et al., 2000, 2001) and provide a good tool for investigating not only the pathogenesis of this disease, but also the intracellular mechanisms underline P-Tau-synaptopathy (Buccarello et al., 2017a).

The P301L's tauopathy showed a clear sex difference: females were more severely affected than male mice, resulting in a more severe tau-synaptopathy and a higher mortality rate in female vs male tg mice (Buccarello et al., 2017a). This is particularly interesting because, in human, the dementia incidence is 16% higher in females than males and, in addition, females with dementia or with psychotic disorders had significantly higher level of phosphorylated Tau compared to males (Koppel et al., 2014; Murray et al., 2014), supporting the theory of sexual dimorphism in this brain pathology. Here we correlate the P301L's synaptopathy to: 1 – the behavioral impairments, the cognitive and locomotor defects, and 2 – the activation of stress JNK signaling pathway and the P-Tau accumulation at the dendritic spine level. We find a genotypic effect on behavioral tests and, importantly, females presented greater cognitive and locomotor impairments than male tg mice, confirming the strong synaptic damage previously detected in P301L females mice (Buccarello et al., 2017a). These data indicate, for the first time, that JNK is involved in P301L synaptopathy and the synaptic dysfunction is stronger in female than male tg mice. These results suggest that JNK is playing a key role in Tau-induced synaptic injury and underline once more the importance of sex/gender therapies against neurodegenerative diseases.

EXPERIMENTAL PROCEDURES

Mice

Male and female P301L-tg mice were purchased from Taconic Laboratories, USA, and bred on a B6D2F1 background in the IRCCS Mario Negri Institute of Pharmacological Research in a Specific Pathogen free (SPF) facility with a regular 12:12-h light/dark cycle (lights on 07:00 a.m.), at a constant room temperature of $22 \pm 2^\circ\text{C}$, and relative humidity approximately 55 \pm 10%. As a classic tauopathy model, hemizygous P301L-tg mice carry the mutant form of human tau protein (P301L), which includes four-repeats without amino terminal inserts, and driven by the mouse prion

promoter 6 (MoPrP) (Borchelt and Sisodia, 1996; Borchelt et al., 1996).

P301L-tg and control mice were provisioned with bedding material (hard wood shavings), ad libitum food (Envigo Lab. 2018S Tekland global diet) and water.

All animal experiments were performed according to the national and international laws and policies (EEC Council Directive 86/609, OJ L 358, 1 Dec.12, 1987; NIH Guide for the Care and use of Laboratory Animals, U.S. National Research Council, 2011). The Mario Negri Institute for Pharmacological Research (IRCCS, Milan, Italy) Animal Care and Use Committee (IACUC) approved the experiments, which were conducted according to the institutional guidelines, which are in compliance with Italian laws (D.L. no. 116, G.U. suppl. 40, Feb. 18, 1992, Circular No. 8, G.U., July 14, 1994). The scientific project was approved by Italian Ministry of Health (Permit Number: 71/2014B). At the age of 15 months, all animals performed behavioral tests and, 24 hours after the tests, mice were sacrificed for biochemical analysis.

Behavioral tests: open-field test and spontaneous locomotor activity

The Open-Field test (OFT) is used to examine the general locomotion, as well as exploration activities, and consequent level of anxiety by exposing mice to a novel and open space (Crawley, 1999; Seibenhener and Wooten, 2015; Walsh and Cummins, 1976). We used a gray Perspex OF box (40 \times 40 \times 40 cm) with the floor divided into 25 (8 \times 8 cm) squares. After allowing the animals to acclimatize to the testing room for 30 min, the mice were placed into the behavioral room in order to decrease their reactions to a novel environment. Mice were placed into the center of the floor defined as a 'starting point' and their behavior video-recorded for 5 min. This short time period was chosen to avoid further stress to tg mice. The parameters analyzed as measure of spontaneous locomotor activity, exploratory activity and state of anxiety were: the duration of locomotion divided into the number of internal (the nine central squares) and external (the sixteen peripheral squares) square crossed, the time spent in the central and external area of the open field, the number and duration of rearing (standing on the hind paws with the front limbs either against the wall or freely in the air (Streng, 1974); the number and duration of self-grooming (rubbing the body with paws or mouth and rubbing the head with paws). The animals in immobile state longer than 4 minutes were excluded from statistical analysis. The time window between the OF and the NORT was of 24hrs (Buccarello et al., 2017a) and we used $n = 10$ animals for each experimental group.

Behavioral tests: novel-object recognition test

The novel-object recognition test (NORT) is a memory test that relies on spontaneous animal behavior (Clarke et al., 2010; Ennaceur and Delacour, 1988) without the need for stressful elements such as food or water deprivation or foot-shock (Antunes and Biala, 2012). The NORT

was conducted in an open-field arena (40 × 40 × 40 cm) with floor divided into 25 squares by black lines; three stimulus objects of similar size were used: a black plastic cylinder (4 × 5 cm), a glass vial with a white cap (3 × 6 cm), and a metal cube (3 × 5 cm). The first phase of the NORT is the *habituation trial* during which the animals were placed in the empty arena for 5 min, and their movements were recorded as the number of line crossings, which provided an indication of locomotion motor activities. In the next day, mice were re-placed in the same arena containing two identical objects (familiarization phase/second phase). The objects were randomly selected to avoid bias among animals and between groups. Objects and positions were counterbalanced across experiments and behavioral trials. Exploration was recorded in a 10-min trial by an investigator blinded to the genotype and treatment. Sniffing, touching, and stretching the head toward the object at a distance of no more than 2 cm were scored as object investigation. In the Novel object phase, twenty-four hours later (3 phase), mice were placed again in the arena containing two objects: one already presented during the familiarization phase (familiar object) and a new different one (novel object). The time spent exploring the two objects was recorded for 10 min; animals with a time of investigation equal to 0 or minor to 2 s were excluded from the statistical analysis. Results were expressed as percentage time of investigation on objects per 10 min or as discrimination index (DI), i.e., (seconds spent on novel – seconds spent on familiar)/(total time spent on objects). Animals with no memory impairment spent a longer time investigating the novel object, giving a higher DI. In order to avoid further stress to tg mice, we decided to use the OF test as habituation trial for the Novel object recognition test and we used $n = 10$ animals for each experimental group.

192 Subcellular fractionation (TIF)

193 After the behavioral test, animals were sacrificed and
194 brains were removed for biochemical analysis.
195 Subcellular fractionation was performed as reported in
196 the literature with minor modifications for both cortex
197 and hippocampus from P301L-tg mice (Buccarello et al.,
198 2017a). Briefly, cortex and hippocampi were dissected
199 and homogenized in 0.32 M ice-cold sucrose buffer
200 containing the following (in mM): 1 HEPES, 1 MgCl₂, 1
201 EDTA, 1 NaHCO₃ and 0.1 PMSF, at pH 7.4, in the pres-
202 ence of a complete set of protease inhibitors (Complete;
203 Roche Diagnostics, Basel, Switzerland) and phos-
204 phatases inhibitors (Sigma, St. Louis, MO, USA). Sam-
205 ples were centrifuged at 1000×*g* for 10 min. The
206 resulting supernatant (S1) was centrifuged at 13000×*g*
207 for 15 min to obtain a crude membrane fraction (P2 frac-
208 tion). The pellet was resuspended in 1 mM HEPES plus
209 protease and phosphatase inhibitor in a glass potter and
210 centrifuged at 100000×*g* for 1 h. The pellet (P3) was
211 resuspended in buffer containing 75 mM KCl and 1% Tri-
212 ton X-100 and centrifuged at 100000×*g* for 1 h. The final
213 pellet (P4) referred to as TIF was homogenized in a glass
214 potter in 20 mM HEPES and stored at –80 °C until
215 processing.

Western blot

Protein concentrations were quantified using the Bradford Assay (Bio-Rad Protein Assay 500–0006, Munchen, Germany) 5 μg of TIF extracted proteins were separated by 10% SDS polyacrylamide gel electrophoresis. PVDF membranes were blocked in Tris-buffered saline (5% non-fat milk powder, 0.1% Tween20, 1 h, room temperature). Primary antibodies were diluted in the same buffer (incubation overnight, 4 °C) using: c-Jun (cat. #9165, 1:1000, Cell Signaling Technology, Danvers, MA, USA), P-c-Jun [Ser63] (cat. #9164, 1:1000, Cell Signaling Technology, Danvers, MA, USA), P-JNK (cat. #9251, 1:1000, Cell Signaling Technology, Danvers, MA, USA), JNK (cat. #9252, 1:1000, Cell Signaling Technology), anti-postsynaptic density protein 95 PSD95 (cat. #10009506, 1:2000, Cayman Chemical Company), anti phospho-PSD95 (cat. #10011435, 1:2000, Cayman Chemical Company), Caspase 3 (Anti-Caspase-3 cat. #AB13847, 1:500, AbCAM), anti-Drebrin (cat. # AB10140, 1:1000, Millipore), anti P-Tau (cat. #MABN388, 1:1000, Millipore, Billerica, MA, USA), anti-Actin (cat. #MAB1501, 1:5000, Millipore, Billerica, MA, USA) and at least six independent experiments were performed. Blots were developed using horseradish peroxidase-conjugated secondary antibodies (Santa Cruz Biotechnology) and the Clarity Western ECL Blotting Substrates (Bio-Rad). Western blots were quantified by densitometry using ImageLab 6.0 software (software associated to ChemiDoc MP images, Bio-Rad) and was based on at least three independent experiments, using $n = 10$ animals for each experimental group.

Statistical analysis

Statistical analysis was performed using Graph Pad Prism 6 program. All data were analyzed using Two-way ANOVA, followed by Tukey's *post hoc* test, and were expressed as mean ± SEM with a statistical significance given at $p < 0.05$. For the calculation of the “Sample size” estimated with the following formula: $n = 2\sigma^2f(a, \beta)/\Delta^2$, for the behavioral analysis the number calculated by experimental group is $n = 10$ and for biochemical analysis $n = 6$.

RESULTS

The cognitive deficits and locomotor impairments in P301L-tg mice

To correlate P301L-tg's synaptopathy, previously described (Buccarello et al., 2017a), with functional defects, we examined cognitive and locomotor impairments in this mouse model, analysing separately females and male mice. The P301L-tg's females and male mice were assessed with two different tests to reveal their impairments compared to control mice. In the Novel Object Recognition test (NORT), P301L-tg showed strong cognitive deficits compared to ctr mice (evaluating discrimination index: DI). In fact, P301L-tg exhibited severe memory deficits, as they spent less time, compared to control mice, investigating the novel object compared to

273 the familiar object (Two-way ANOVA, $p < 0.05$,
274 $p < 0.001$; Fig. 1A). Therefore, females were more
275 severely affected than males, having a lower discrimina-
276 tion index compared to male mice (Two-way ANOVA,
277 $p < 0.05$, Fig. 1A), while, there was no statistically signifi-
278 cant difference between male and female in ctr mice (see
279 Fig. 1A).

280 Concerning the valuation of locomotor activity, a
281 significant genotype effect on these performances was
282 observed (Two-way ANOVA, $p < 0.01$, $p < 0.001$;
283 Fig. 1B-D), as expected. In particular, female P301L-tg
284 showed a greater decrease in the total number of
285 crossing ($p < 0.001$; Fig. 1B) as well as in the number
286 of internal and external crossing (Two-way ANOVA,
287 $p < 0.01$, $p < 0.001$; Fig. 1C-D) compared to P301L-tg
288 male. There was no statistically significant difference
289 between male and female ctr mice (see Fig. 1B-D).

290 The cognitive and locomotor impairments presented a
291 clear sex bias, this well correlated with PSD biochemical
292 markers deregulation previously detected (Buccarello
293 et al., 2017a).

The activation of JNK signaling pathway in P301L-tg mice

294 We here analyzed the JNK involvement in P301L-tg
295 pathology in total homogenates. To quantify JNK
296 activation, we measured both the action of JNK on its
297 elective target c-Jun (P-c-Jun/c-Jun ratio) and the
298 phosphorylation state/activation of the kinase itself (P-
299 JNK/JNK ratio). In the cortex and hippocampus, P-c-
300 Jun/c-Jun and P-JNK/JNK ratios were significant higher
301 in P301L-tg compared to ctr mice (see Fig. 2A-D),
302 indicating the activation of the stress-JNK signaling in tg
303 mice. In particular, in the cortex we observed an
304 increased level of P-c-Jun/c-Jun ratio in males (Two-
305 way ANOVA, $p < 0.05$, Fig. 2A-B) and females P301L-
306 tg (Two-way ANOVA, $p < 0.001$, Fig. 2A-B) vs ctr mice
307 and a strong increase of P-JNK/JNK ratio (Two-way
308 ANOVA, $p < 0.001$, Fig. 2A-B) in both sexes compared
309 to ctr mice. In the hippocampus, P-c-Jun/c-Jun and P-
310 JNK/JNK ratios were higher in both sexes of P301L-tg
311 in comparison with ctr mice (Two-way ANOVA,
312 $p < 0.01$, $p < 0.001$; Fig. 2C-D). As for the behavioral
313
314

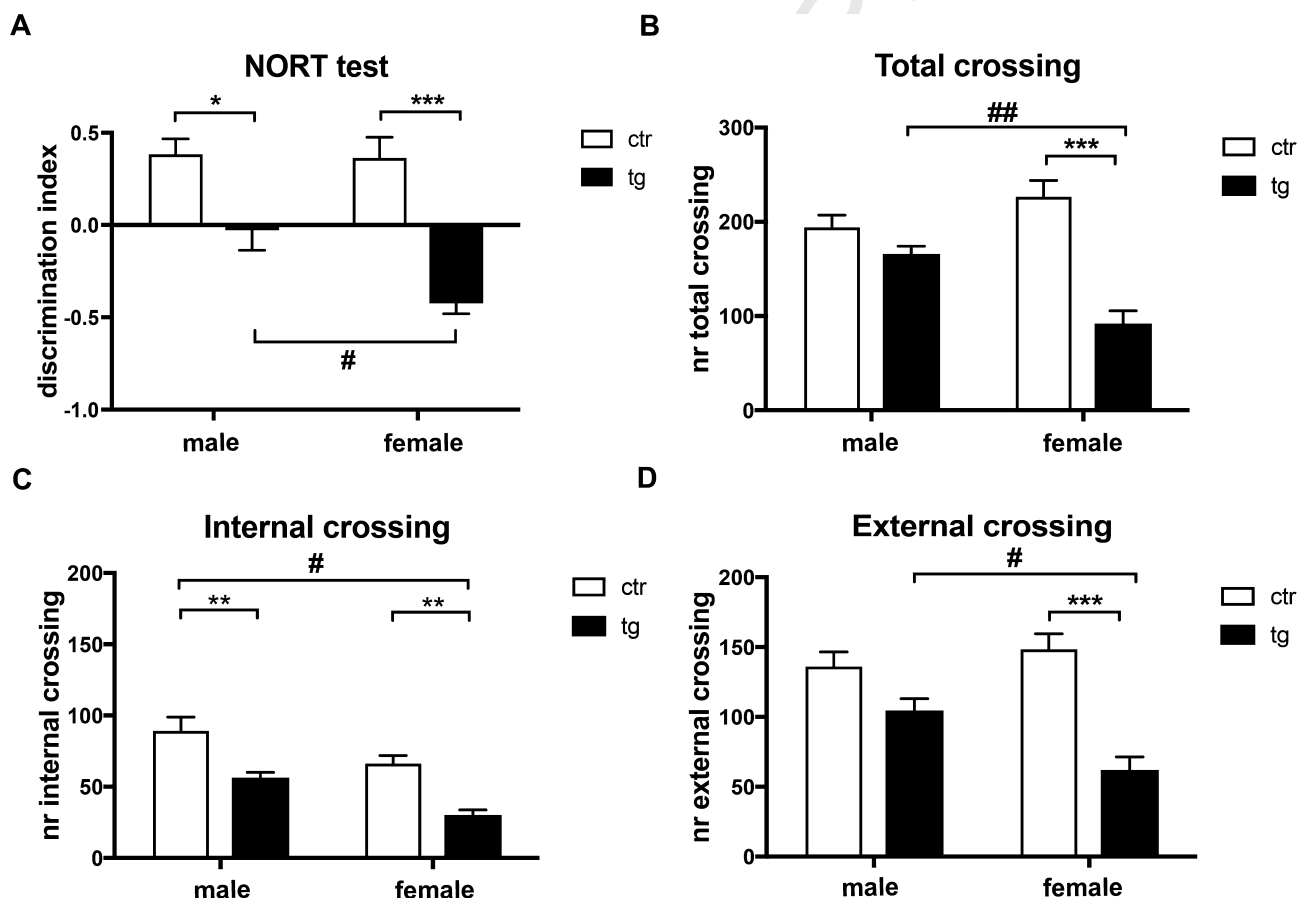


Fig. 1. Cognitive and locomotor deficits in P301L-tg mice. A) The Novel Object Recognition Test. Histograms indicate the time percentage (mean ± SEM) of investigation on the familiar and novel objects performed by female and male ctr and P301L-tg mice. There is a significant reduction of discrimination index in both male and female tg mice compared with the age-matched ctr mice, with a greater DI decrease in female vs. male tg mice. Significant relative to control $^*p < 0.05$, $^{***}p < 0.001$; tg female vs. male $^{\#}p < 0.05$. B-D) The Open Field Test. Histograms represent the locomotor activity in 15-months-old female and male ctr and P301L-tg mice. Both male and female tg mice had a significant reduction of locomotor performance if compared with ctr mice, with a greater decrease in female vs male tg mice. Total crossing: significant relative to control $^{***}p < 0.001$; tg female vs male $^{###}p < 0.01$. Internal crossing: significant relative to control $^{**}p < 0.01$; tg female vs male $^{\#}p < 0.05$. External crossing: significant relative to control $^{***}p < 0.001$; tg female vs male $^{\#}p < 0.05$ [$n = 10$]. Two-way ANOVA, Tukey's post-hoc test. Data were shown as mean ± SEM.

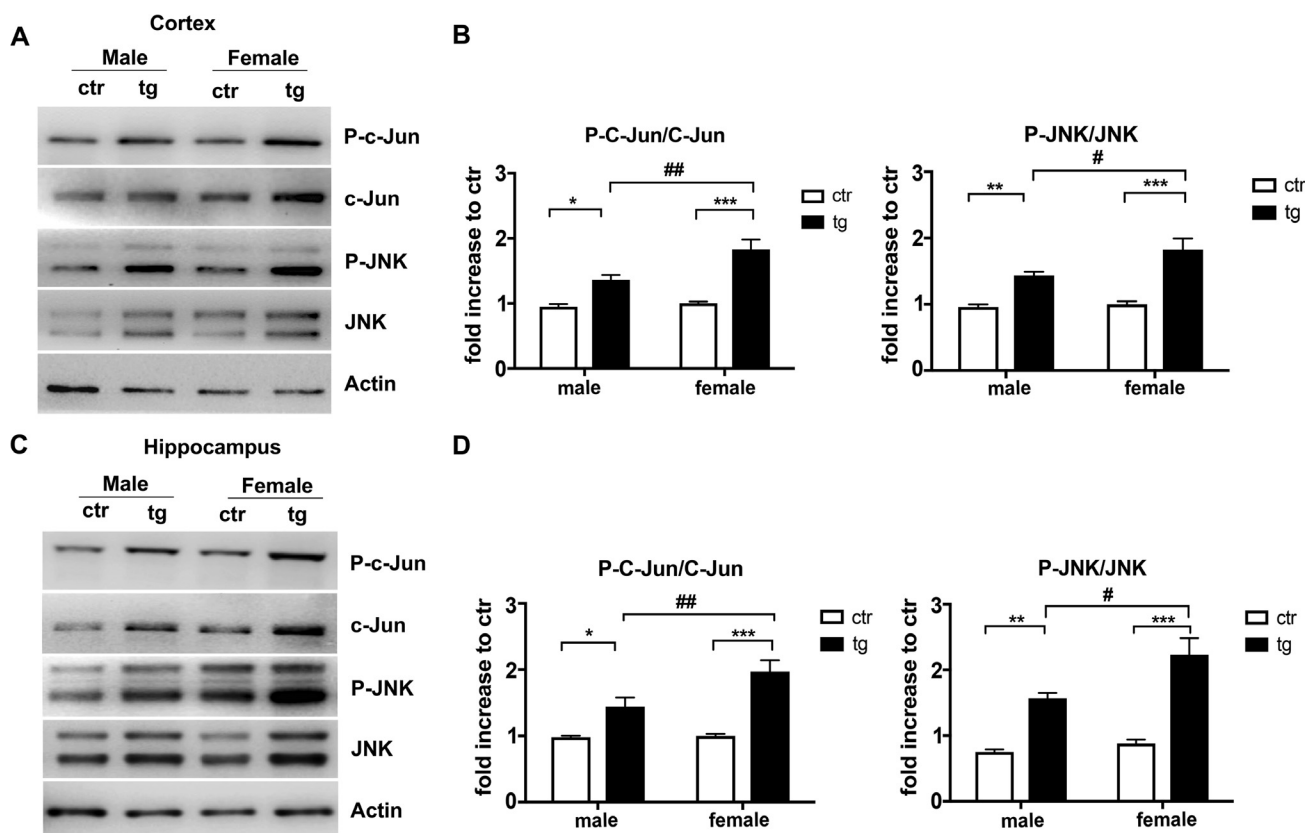


Fig. 2. Characterization of JNK pathway in the cerebral cortex and hippocampus of P301L-tg mice. A-C) Western blots and (B-D) relative quantifications showing P-JNK, JNK, P-c-Jun and c-Jun in the cerebral cortex and hippocampus from 15-month-old male and female ctr and P301L-tg mice. P-JNK/JNK and P-c-Jun/c-Jun ratios were increased in both male and female tg mice compared to the age-matched ctr mice in both brain areas analyzed. Considering the sex bias in both brain areas, P-c-Jun/c-Jun and P-JNK/JNK ratios were significant increase in female vs male tg mice. Cortex: significant relative to control * $p < 0.05$, *** $p < 0.001$, tg female vs. male # $p < 0.05$, ## $p < 0.01$. Hippocampus: significant relative to control ** $p < 0.01$, *** $p < 0.001$, tg female vs. male # $p < 0.05$, ## $p < 0.01$ [$n = 10$]. Two-way ANOVA, Tukey's post-hoc test. Data are shown as mean \pm SEM.

315 tests, we separated females and male mice to study the
316 sex difference in JNK pathway activation. In the cortex,
317 the P-c-Jun/c-Jun and the P-JNK/JNK ratios were
318 significant increase in females (Two-way ANOVA, P-c-
319 Jun/c-Jun $p < 0.01$, P-JNK/JNK $p < 0.05$, Fig. 2A-B)
320 compared to male tg mice. In the hippocampus, the P-c-
321 Jun/c-Jun (Two-way ANOVA, $p < 0.01$, Fig. 2C-D) and
322 P-JNK/JNK (Two-way ANOVA, $p < 0.05$, Fig. 2C-D)
323 ratios were higher in female vs male tg mice as well.
324 Thus, in summary the stress signaling JNK pathway is
325 more activated in females P301L-tg mice in total
326 homogenates.

327 P-Tau- and Caspase-3 activation in P301L-tg mice

328 Tau is a direct JNK's target (Ploia et al., 2011) and the
329 hyper-phosphorylation of Tau is the main pathological
330 feature in tauopathy. The total P-Tau (P-Tau_{tot}) level
331 was measured in order to correlate this parameter to
332 JNK pathway activation in this model. The P301L-tg mice
333 presented a significant increased level of P-Tau_{tot} com-
334 pared to ctr mice in both cortex and hippocampus (Two-
335 way ANOVA, $p < 0.05$ and $p < 0.001$, see Fig. 3A-D).
336 In addition, P-Tau_{tot} level was higher in female vs male
337 tg mice in both brain areas analyzed (Two-way ANOVA,

$p < 0.05$, Fig. 3A-D). Thus, females showed higher P-
338 Tau_{tot} level compared to male P301L-tg mice, as previ-
339 ously reported by using different anti-bodies against
340 specific sites of Tau phosphorylation (Buccarello et al.,
341 2017a). Moreover, also caspase-3 is a direct JNK's target
342 and it is implicated in neurodegenerative processes as
343 well (D'Amelio et al., 2011; Sclip et al., 2014). Thus, we
344 analyzed the activation of caspase-3 (cleaved-caspase-
345 3) in P301L-tg total homogenates: cleaved-caspase-3
346 level was significantly higher in P301L-tg compared to
347 ctr mice in both cortex and hippocampus (Two-way
348 ANOVA, $p < 0.001$, Fig. 3A-D). Concerning the sexual
349 dimorphism, the cleaved-caspase-3 level was higher in
350 female vs male tg mice in both brain areas (Two-way
351 ANOVA, $p < 0.01$ and $p < 0.05$, Fig. 3B-D). As a result,
352 there is a sex-genotype effect on total P-Tau and cleaved
353 caspase-3 levels in P301L-tg mice.
354

355 The dendritic spine pathology: JNK activation

356 We analyzed at the dendritic spine level the JNK
357 activation to characterize the synaptic dysfunctionality/
358 spine pathology of P301L-tg mice, never studied yet in
359 this mouse model. The P-JNK/JNK ratio was
360 significantly increased in P301L-tg compared to ctr mice

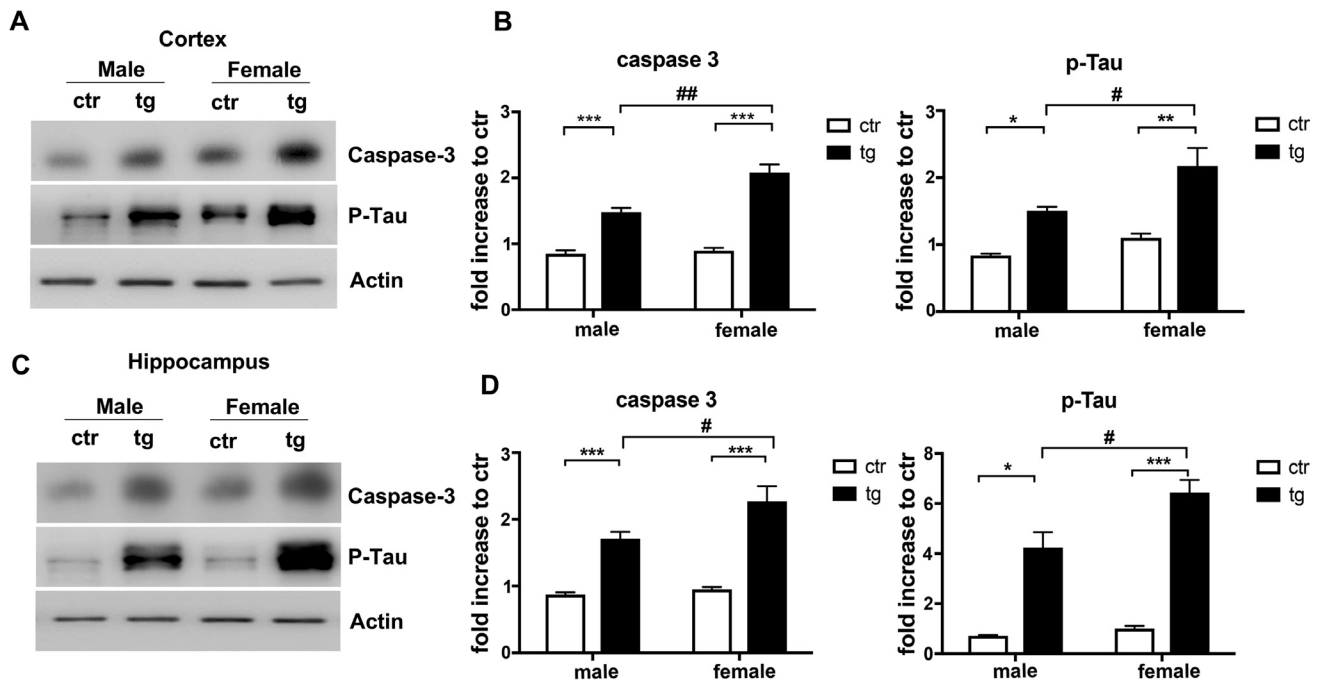


Fig. 3. Caspase-3 activation and P-Tau deposition in P301L-tg mice. (A-C) Western blots and (B-D) relative quantifications showing cleaved-caspase-3 and P-Tau_{tot} in the cerebral cortex and hippocampus from 15-month-old male and female ctr and P301L-tg mice. The cleaved-caspase-3 and P-Tau_{tot} levels were increased in both males and female tg mice compared to ctr mice in both the cortex and hippocampus, with a greater increase in females vs male tg mice in both brain areas analyzed. For cortex: significant relative to control * $p < 0.05$, ** $p < 0.01$, *** $p < 0.001$; tg female vs male # $p < 0.05$ and ## $p < 0.01$. For Hippocampus: significant relative to control * $p < 0.05$, *** $p < 0.001$, tg female vs male # $p < 0.05$ [$n = 10$]. Two-way ANOVA, Tukey's post-hoc test. Data are shown as mean \pm SEM.

361 in the post-synaptic elements (see Fig. 4A-D), indicating
 362 that also at this level, the JNK signaling is powerfully
 363 activated. In particular, in the cortex, we observed a
 364 strong increase of P-JNK/JNK ratio in both sexes (Two-
 365 way ANOVA, $p < 0.001$, Fig. 4A-B) compared to ctr
 366 mice and, in the hippocampus, the P-JNK/JNK ratio was
 367 higher in males (Two-way ANOVA, $p < 0.01$; Fig. 4C-D)
 368 and females (Two-way ANOVA, $p < 0.001$; Fig. 4C-D)
 369 compared to ctr mice. We confirmed the sexual
 370 dimorphism previously observed, finding a stronger JNK
 371 activation in female vs male tg mice (Two-way ANOVA,
 372 $p < 0.001$, Fig. 4A-D). To link the spine dysfunctionality
 373 to the pathological Tau species, we studied P-Tau_{tot}
 374 missorting at the dendritic spine level. The P-Tau_{tot}
 375 level was significantly higher in tg vs control mice in both
 376 brain areas analyzed (Two-way ANOVA, cortex:
 377 $p < 0.05$ and $p < 0.001$, hippocampus: $p < 0.001$,
 378 Fig. 4A-D), and females showed higher P-Tau_{tot} level vs
 379 male tg (Two-way ANOVA, cortex: $p < 0.05$ and
 380 hippocampus: $p < 0.001$, Fig. 4A-D), indicating a sex
 381 bias. In addition, we measured the phosphorylation of
 382 JNK on PSD95, a direct JNK's target and the most
 383 abundant scaffold protein of the PSD region. We
 384 already demonstrated PSD95 altered level in this model
 385 (Buccarello et al., 2017a); however, here we measured
 386 the P-PSD95/PSD95 ratio, studying the phosphorylation
 387 of PSD95 specifically mediated by JNK. The P-PSD95/
 388 PSD95 ratio was higher in P301L-tg compared to ctr
 389 mice, indicating a significant genotypic difference in the
 390 cortex as well as in the hippocampus (Two-way ANOVA,
 391 cortex: $p < 0.01$, $p < 0.001$ and hippocampus:

392 $p < 0.001$; Fig. 4A-D). Importantly, dendritic spines pre-
 393 sented a higher increase of P-PSD95/PSD95 ratio in
 394 female vs male tg mice in both brain areas (Two-way
 395 ANOVA, cortex: $p < 0.05$ and hippocampus: $p < 0.001$,
 396 Fig. 4A-D), denoting that there is a significant sex differ-
 397 ence. To further characterize the spine pathology and
 398 its correlation with the JNK stress pathway, we analyzed
 399 the also the other JNK target, measuring the cleaved-
 400 caspase-3 level. Such as in the whole homogenate, we
 401 found a significant genotypic difference of its level: in fact,
 402 cleaved-caspase-3 level is higher, in both males and
 403 females P301L-tg mice compared to ctr mice in both brain
 404 areas analyzed (Two-way ANOVA, cortex and hippocam-
 405 pus: $p < 0.05$, $p < 0.001$, Fig. 4A-D), proving a genotypic
 406 effect. Concerning the sexual dimorphism, we observed
 407 an increased cleaved-caspase-3 level in females com-
 408 pared to male P301L-tg mice (Two-way ANOVA,
 409 $p < 0.05$, $p < 0.001$, Fig. 4A-D) in both brain areas
 410 examined. At the dendritic spine level, there was a sex
 411 effect on the caspase-3 activation in P301L-tg mice. We
 412 then examined Drebrin, an actin-binding protein highly
 413 concentrated within dendritic spines (Koganezawa et al.,
 414 2017), implicated in spine morphological changes. The
 415 Drebrin level was lower in tg compared to ctr mice in both
 416 brain areas analyzed (Two-way ANOVA, cortex:
 417 $p < 0.001$; hippocampus: $p < 0.01$ and $p < 0.001$,
 418 Fig. 4A-D), indicating smaller or less-plastic spines.
 419 Intriguingly, females showed lower Drebrin level vs male
 420 tg mice (Two-way ANOVA, cortex and hippocampus:
 421 $p < 0.001$, Fig. 4A-D), confirming the sexual dimorphism
 422 in P301L mouse model.

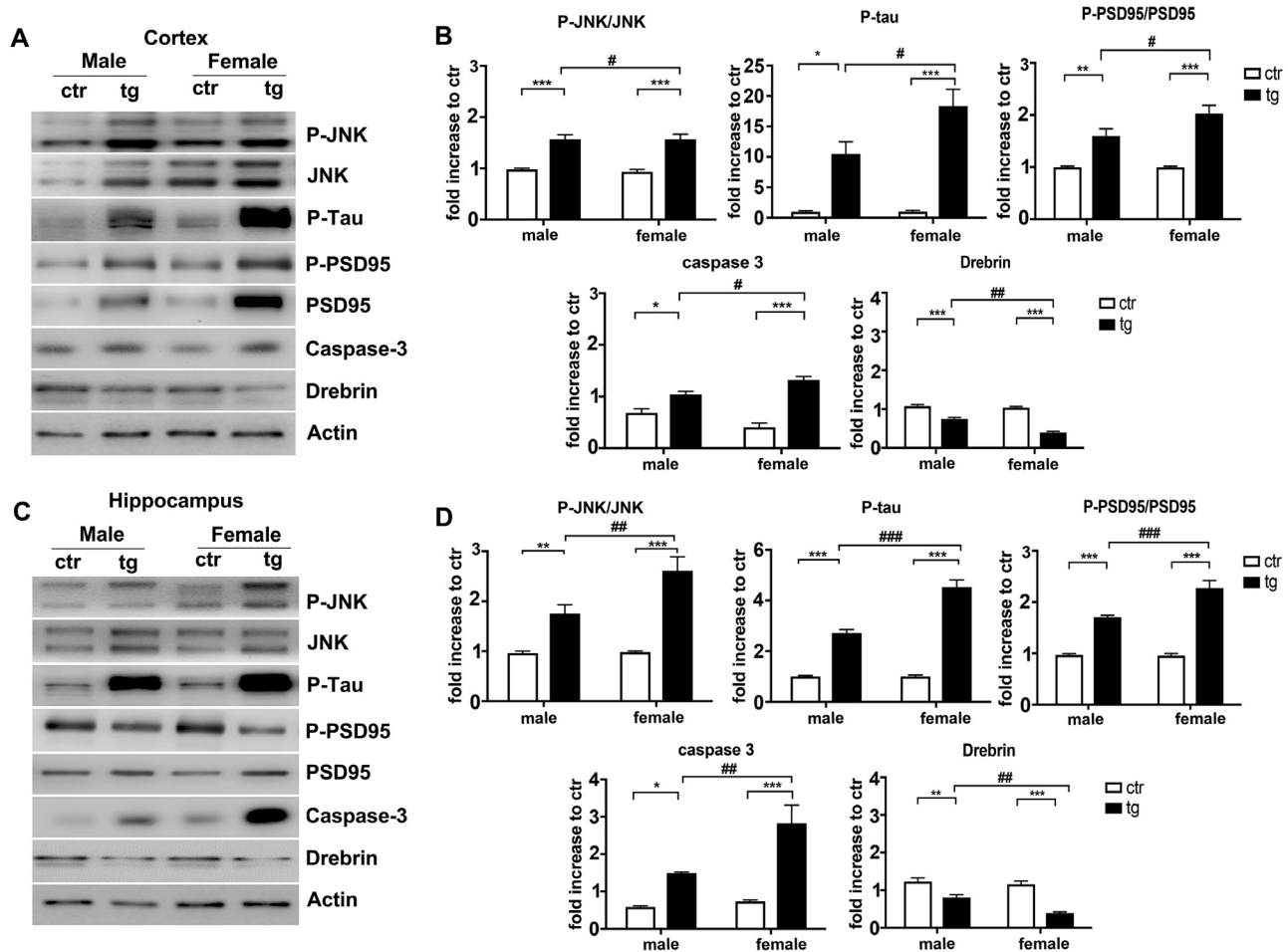


Fig. 4. The P301L-tg synaptopathy. A-C) Western blots and (B-D) relative quantifications performed on the TIF fraction showed in cortex and in hippocampus a significant increase of P-JNK/JNK and P-PSD95/PSD95 ratios in both females and male tg compared to ctr mice. It was found also in both brain areas a significant increase of P-Tau_{tot} and cleaved-Caspase-3 level in both male and female tg mice compared to ctr mice and a strongly increase in female vs male tg mice. Drebrin level was decreased in male and female tg vs ctr mice in both the cortex and hippocampus, with a powerful reduction in females vs male tg mice in both brain areas analyzed. For P-JNK/JNK and P-PSD95/PSD95 ratios, Cortex: significant relative to control $^{**}p < 0.01$, $^{***}p < 0.001$, tg female vs male $^{\#}p < 0.05$; Hippocampus: significant relative to control $^{**}p < 0.01$, $^{***}p < 0.001$; tg female vs. male $^{\#\#}p < 0.01$, $^{\#\#\#}p < 0.001$. For Caspase 3, P-Tau_{tot} and Drebrin, cortex: significant relative to control $^{*}p < 0.05$, $^{***}p < 0.001$; tg female vs male $^{\#}p < 0.05$, $^{\#\#}p < 0.01$; Hippocampus: significant relative to control $^{*}p < 0.05$, $^{**}p < 0.01$, $^{***}p < 0.001$, tg female vs. male $^{\#\#}p < 0.01$ [$n = 10$]. Two-way ANOVA, Tukey's post-hoc test. Data are shown as mean \pm SEM.

DISCUSSION

423

424 The main pathological hallmark of tauopathies is
 425 hyperphosphorylated Tau aggregates (NFTs) in the
 426 somato-dendritic compartment (Avila et al., 2004;
 427 Gendron and Petrucelli, 2009); more recently, P-Tau species
 428 has been identified also at the dendritic spine level
 429 (Haass and Mandelkow, 2010; Hoover et al., 2010;
 430 Menkes-Caspi et al., 2015). In particular, P301L-tg mice
 431 presented P-Tau and Tau missorted at the PSD region
 432 and this has been previously associated with PSD marker
 433 reduction levels (Buccarello et al., 2017a; Hoover et al.,
 434 2010), suggesting a role of P-Tau in spine pathology.
 435 Likewise, in primary neurons derived from P301L-tg mice,
 436 the mutant Tau (P-Tau) located to dendritic spines more
 437 than in control mice (Hoover et al., 2010). Thus, P-Tau
 438 accumulated into dendritic spines, but its pathological
 439 role, at this level, is not clear yet.

440 We find a correlation between behavioral impairments
 441 (cognitive and locomotor tests NORT and OF) and
 442 synaptic pathology (biochemical marker changes and
 443 the accumulation of toxic P-Tau) in P301L-tg mice. The
 444 behavioral tests demonstrated cognitive and locomotor
 445 impairments and, importantly, in both tasks the
 446 pathology was more severe in females compared to
 447 male tg mice. The functional analysis corroborates the
 448 previous metabolic results, confirming the most severe
 449 pathological phenotype in tg female associated to a
 450 significant body weight decrease and a lower
 451 percentage of survival rate compared to male mice
 452 (Buccarello et al., 2017a). In agreement with our data,
 453 Kandimalla and co-workers (Kandimalla et al., 2018)
 454 found that hippocampal learning/memory, motor learning
 455 and coordination were impaired in P301L mice, highlight-
 456 ing as hippocampal accumulation of P-Tau is responsible
 457 for abnormal mitochondrial dynamics, dysmorphogenesis

of dendritic spines and behavioral defects in this tauopathy mouse model.

The functional data on behavioral impairments completed a coherent picture, in which, females are more severely affected than male mice. Concerning the pathological mechanism that underlies hyperphosphorylated-Tau and its aggregates species in P301L, we investigated the possible involvement of the stress JNK signaling pathway. Notably, JNK not only hyperphosphorylates Tau (Buccarello et al., 2017b; Orejana et al., 2013; Ploia et al., 2011), but it is also a key player in the AD's synaptic pathology, indicating a possible role of this stress pathway in this tauopathy model too. Here, analysing the JNK activation using a double approach for its quantification (evaluating the phosphorylation of JNK kinase itself and of its main target c-Jun), we proved a powerful JNK activation in P301L-tg mice.

Importantly, phospho-JNK was associated to hyperphosphorylated Tau in human samples (Atzori et al., 2001), this gives a translational value to JNK role in Human. Moreover, neuropathological and biochemical findings reported in patients affected by frontotemporal dementia associated with a P310L, Tau accumulation in neurons associated with increased expression of different kinases, linked with tau phosphorylation such as p38, cdk5 and GSK-3 beta (Ferrer et al., 2003).

P-Tau_{mut} and P-JNK increased levels may be due to a wide range of stress pathway activations, among these ER and mitochondria play important roles in this cascade. How P-Tau_{mut} triggers downstream JNK activation is not clear yet. We speculate that this may be due to microtubule disaggregation induced by the hyperphosphorylation of Tau, that leads to c-Jun N-terminal kinase-interacting protein 1 (JIP1) detachment from microtubules. JIP1 is a scaffold protein involved in focusing and accelerating JNK activity; if JIP1 is free from the microtubules, can link JNK and accelerate and focus its phosphorylation (inducing and increasing P-JNK level). Further experiments are needed to investigate this issue.

In more details, in P301L mice P-JNK is higher in hippocampus (hippocampus 28% more than cortex) compared to the cortex, suggesting that these two brain areas are differentially affected by the Tau-pathology. This difference has already been previously reported in this transgenic mouse model (Buccarello et al., 2017b). Interestingly, comparing the JNK activation between sexes in whole homogenate, in both brain areas, we found a sex bias underlying a stronger activation of JNK in female vs male P301L-tg mice. To better clarify the JNK role in tauopathy, we analyzed different JNK targets implicated in neurodegenerative processes (Antoniu et al., 2011; Borsello et al., 2003; Repici and Borsello, 2006). In whole homogenate, we studied the elective JNK target c-Jun and cleaved-caspase-3, a direct JNK's target and an important executor in the apoptotic degenerative pathway (D'Amelio et al., 2011; Scip et al., 2013) implicated in neuronal death, these are significantly higher in tg compared to ctr mice. Notably, the c-Jun and cleaved-caspase-3 levels are higher in female vs male

P301L-tg mice, indicating that the death pathway activation is prominent in female vs male tg mice, as expected. Therefore, females are more severely affected by tauopathy than male mice in P301L mouse model (Buccarello et al., 2017a; Hunsberger et al., 2014; Katsuse et al., 2006) as well as in human patients (Narasimhan et al., 2017).

Being synaptic pathology a key feature in many brain diseases, we focus on studying the mechanism of spine degeneration. We examined JNK activation at the dendritic spine level, since in polarized cell, like neurons, the localization/cellular compartments of the kinase activity are even more important.

In addition, we focused on studying the mechanism of spine pathology. JNK is strongly activated at the spine level as well. This according to our knowledge is the first data indicating JNK involvement in Tau-induced spine injury.

In this context, P-JNK/JNK ratio was increased in P301L-tg compared to ctr mice, and its level was significantly higher in females vs male P301L-tg, indicating an important sexual dimorphism. Notably, we investigated also the P-Tau_{tot} at the dendritic spine level to correlate toxic Tau species with JNK activation at the dendritic spine. The P-Tau_{tot} level presented a sex-genotype effect, in line with JNK activation.

Concerning the JNK targets at this level, PSD95 and cleaved-caspase-3 showed an increased in P301L-tg compared to ctr mice. Importantly, females exhibited higher levels in comparison with male P301L-tg, indicating an important sexual dimorphism. Finally, the Drebrin marker is in line with P-Tau-induced spine pathology: in fact, P301L-tg mice showed lower Drebrin level compared to ctr mice and females showed a further reduction than male tg mice. The decreased Drebrin level indicates smaller or less-plastic dendritic spines and this was more pronounced in females, indicating a stronger impairment of their synapses. All together these data suggest that dendritic spine pathology presents an important sex dimorphism: females showed a higher activation of JNK and its targets with a lower Drebrin level revealing a more severe dendritic spine dysfunction/loss in female vs male P301L-tg mice. Notably, the stronger synaptopathy in female vs male tg mice is well correlated with the severe cognitive/locomotor impairments observed in females.

Summarizing, these results suggest that the synaptic dysfunction and memory impairments are caused by abnormal accumulation of P-Tau that this is associated to JNK signaling pathway activation at the spine level, which could be targeted by inhibitory drugs to tackle spine pathology in many different brain diseases.

However how Tau mutation in P301L correlated with the stress JNK pathway activation is not clear yet, since JNK is a kinase activated by many different stressors.

Importantly, the sex bias described for JNK signaling is a very interesting aspect, going in the direction of the gender differences found in many brain diseases. It will be fundamental now to verify the translational value of these results studying patient's tissues, since JNK

580 could be a new target and also an important predictive
581 biomarker of synaptopathy. In fact, recently encouraging
582 evidences had showed that JNK3 is detected in MCI
583 and AD liquors as a new indicator of dementia
584 (Gourmaud et al., 2015).

585 CONCLUSION

586 JNK sexual dimorphic activation can have important
587 implications for future target therapeutic directions and
588 underlines the need of personalized medicine, an
589 important aspect of which is the sex and gender
590 differences, which are still underestimate.

591 ACKNOWLEDGMENTS

592 The authors gratefully acknowledge Prof. C. Domeneghini
593 and J. Baggott kindly edited the text.

594 CONFLICTS OF INTEREST

595 The authors declare no actual or potential conflicts of
596 interest.

597 GRANT SUPPORT

598 This work was supported by ADDF (Alzheimer's Drugs
599 Discovery Foundation) USA grant to Tiziana Borsello.

600 REFERENCES

601 Antoniou X, Falconi M, Di Marino D, Borsello T (2011) JNK3 as a
602 therapeutic target for neurodegenerative diseases. *J Alzheimers*
603 *Dis* 24:633–642.
604 Antunes M, Biala G (2012) The novel object recognition memory:
605 neurobiology, test procedure, and its modifications. *Cogn Process*
606 13:93–110.
607 Atzori C, Ghetti B, Piva R, Srinivasan AN, Zolo P, Delisle MB, Mirra
608 SS, Migheli A (2001) Activation of the JNK/p38 pathway occurs in
609 diseases characterized by tau protein pathology and is related to
610 tau phosphorylation but not to apoptosis. *J Neuropathol Exp*
611 *Neurol* 60:1190–1197.
612 Avila J, Lucas JJ, Perez M, Hernandez F (2004) Role of tau protein in
613 both physiological and pathological conditions. *Physiol Rev*
614 84:361–384.
615 Borchelt DR, Sisodia SS (1996) Loss of functional prion protein: a role
616 in prion disorders? *Chem Biol* 3:619–621.
617 Borchelt DR, Davis J, Fischer M, Lee MK, Slunt HH, Ratovitsky T,
618 Regard J, Copeland NG, Jenkins NA, Sisodia SS, et al. (1996) A
619 vector for expressing foreign genes in the brains and hearts of
620 transgenic mice. *Genet Anal* 13:159–163.
621 Borsello T, Croqueolois K, Hornung J-P, Clarke PGH (2003) N-methyl-
622 d-aspartate-triggered neuronal death in organotypic hippocampal
623 cultures is endocytic, autophagic and mediated by the c-Jun N-
624 terminal kinase pathway. *Eur J Neurosci* 18:473–485.
625 Buccarello L, Grignaschi G, Castaldo AM, Di Giancamillo A,
626 Domeneghini C, Melcangi RC, Borsello T (2017a) Sex Impact
627 on Tau-Aggregation and Postsynaptic Protein Levels in the P301L
628 Mouse Model of Tauopathy. *J Alzheimers Dis* 56:1279–1292.
629 Buccarello L, Scip A, Sacchi M, Castaldo AM, Bertani I, ReCecconi
630 A, Maestroni S, Zerbini G, Nucci P, Borsello T (2017b) The c-jun
631 N-terminal kinase plays a key role in ocular degenerative changes
632 in a mouse model of Alzheimer disease suggesting a correlation
633 between ocular and brain pathologies. *Oncotarget*
634 8:83038–83051.

Clarke JR, Cammarota M, Gruart A, Izquierdo I, Delgado-García JM 635
(2010) Plastic modifications induced by object recognition 636
memory processing. *PNAS* 107:2652–2657. 637
Crawley JN (1999) Behavioral phenotyping of transgenic and 638
knockout mice: experimental design and evaluation of general 639
health, sensory functions, motor abilities, and specific behavioral 640
tests. *Brain Res* 835:18–26. 641
Crimins JL, Rocher AB, Peters A, Shultz P, Lewis J, Luebke JI (2011) 642
Homeostatic responses by surviving cortical pyramidal cells in 643
neurodegenerative tauopathy. *Acta Neuropathol* 122:551–564. 644
Crimins JL, Rocher AB, Luebke JI (2012) Electrophysiological 645
changes precede morphological changes to frontal cortical 646
pyramidal neurons in the rTg4510 mouse model of progressive 647
tauopathy. *Acta Neuropathol* 124:777–795. 648
D'Amelio M, Cavallucci V, Middei S, Marchetti C, Pacioni S, Ferri A,
649 Diamantini A, De Zio D, Carrara P, Battistini L, et al. (2011)
650 Caspase-3 triggers early synaptic dysfunction in a mouse model
651 of Alzheimer's disease. *Nat Neurosci* 14:69–76. 652
Delacourte A, Buée L (2000) Tau pathology: a marker of 653
neurodegenerative disorders. *Curr Opin Neurol* 13:371–376. 654
Ennaceur A, Delacour J (1988) A new one-trial test for 655
neurobiological studies of memory in rats. 1: behavioral data. 656
Behav Brain Res 31:47–59. 657
Ferrer I, Hernández I, Puig B, Rey MJ, Ezquerra M, Tolosa E, Boada
658 M (2003) Ubiquitin-negative mini-pick-like bodies in the dentate
659 gyrus in p301I tauopathy. *J Alzheimers Dis* 5:445–454. 660
Gendron TF, Petrucelli L (2009) The role of tau in neurodegeneration.
661 *Mol Neurodegener* 4:13. 662
Gourmaud S, Paquet C, Dumurgier J, Pace C, Bouras C, Gray F,
663 Laplanche J-L, Meurs EF, Mouton-Liger F, Hugon J (2015)
664 Increased levels of cerebrospinal fluid JNK3 associated with
665 amyloid pathology: links to cognitive decline. *J Psychiatry*
666 *Neurosci* 40:151–161. 667
Haass C, Mandelkow E (2010) Fyn-tau-amyloid: a toxic triad. *Cell*
668 142:356–358. 669
Hoover BR, Reed MN, Su J, Penrod RD, Kotilinek LA, Grant MK,
670 Pitstick R, Carlson GA, Lanier LM, Yuan L-L, et al. (2010) Tau
671 mislocalization to dendritic spines mediates synaptic dysfunction
672 independently of neurodegeneration. *Neuron* 68:1067–1081. 673
Hunsberger HC, Rudy CC, Weitzner DS, Zhang C, Tosto DE,
674 Knowlan K, Xu Y, Reed MN (2014) Effect size of memory deficits
675 in mice with adult-onset P301L tau expression. *Behav Brain Res*
676 272:181–195. 677
Ingram EM, Spillantini MG (2002) Tau gene mutations: dissecting the
678 pathogenesis of FTDP-17. *Trends Mol Med* 8:555–562. 679
Kandimalla R, Manczak M, Yin X, Wang R, Reddy PH (2018)
680 Hippocampal phosphorylated tau induced cognitive decline,
681 dendritic spine loss and mitochondrial abnormalities in a mouse
682 model of Alzheimer's disease. *Hum Mol Genet* 27:30–40. 683
Katsuse O, Lin W-L, Lewis J, Hutton ML, Dickson DW (2006)
684 Neurofibrillary tangle-related synaptic alterations of spinal motor
685 neurons of P301L tau transgenic mice. *Neurosci Lett* 409:95–99. 686
Koganezawa N, Hanamura K, Sekino Y, Shirao T (2017) The role of
687 drebrin in dendritic spines. *Mol Cell Neurosci* 84:85–92. 688
Kopeikina KJ, Polydoro M, Tai H-C, Yaeger E, Carlson GA, Pitstick R,
689 Hyman BT, Spires-Jones TL (2013) Synaptic alterations in the
690 rTg4510 mouse model of tauopathy. *J Comp Neurol*
691 521:1334–1353. 692
Koppel J, Acker C, Davies P, Lopez OL, Jimenez H, Arose M,
693 Greenwald BS, Murray PS, Kirkwood CM, Kofler J, et al. (2014)
694 Psychotic Alzheimer's disease is associated with gender-specific
695 tau phosphorylation abnormalities. *Neurobiol Aging*
696 35:2021–2028. 697
Lewis J, McGowan E, Rockwood J, Melrose H, Nacharaju P, Van
698 Slegtenhorst M, Gwinn-Hardy K, Paul Murphy M, Baker M, Yu X,
699 et al. (2000) Neurofibrillary tangles, amyotrophy and progressive
700 motor disturbance in mice expressing mutant (P301L) tau protein.
701 *Nat Genet* 25:402–405. 702
Lewis J, Dickson DW, Lin WL, Chisholm L, Corral A, Jones G, Yen
703 SH, Sahara N, Skipper L, Yager D, et al. (2001) Enhanced 704

- 705 neurofibrillary degeneration in transgenic mice expressing mutant
706 tau and APP. *Science* 293:1487–1491.
- 707 Menkes-Caspi N, Yamin HG, Kellner V, Spires-Jones TL, Cohen D,
708 Stern EA (2015) Pathological tau disrupts ongoing network
709 activity. *Neuron* 85:959–966.
- 710 Murray PS, Kirkwood CM, Gray MC, Fish KN, Ikonovic MD,
711 Hamilton RL, Kofler JK, Klunk WE, Lopez OL, Sweet RA (2014)
712 Hyperphosphorylated tau is elevated in Alzheimer's disease with
713 psychosis. *J Alzheimers Dis* 39:759–773.
- 714 Narasimhan S, Guo JL, Changolkar L, Stieber A, McBride JD, Silva
715 LV, He Z, Zhang B, Gathagan RJ, Trojanowski JQ, et al. (2017)
716 Pathological tau strains from human brains recapitulate the
717 diversity of tauopathies in non-transgenic mouse brain. *J*
718 *Neurosci*.
- 719 Orejana L, Barros-Miñones L, Aguirre N, Puerta E (2013) Implication
720 of JNK pathway on tau pathology and cognitive decline in a
721 senescence-accelerated mouse model. *Exp Gerontol*
722 48:565–571.
- 723 Ploia C, Antoniou X, Scip A, Grande V, Cardinetti D, Colombo A,
724 Canu N, Benussi L, Ghidoni R, Forloni G, et al. (2011) JNK plays
725 a key role in tau hyperphosphorylation in Alzheimer's disease
726 models. *J Alzheimers Dis* 26:315–329.
- 727 Repici M, Borsello T (2006) JNK pathway as therapeutic target to
728 prevent degeneration in the central nervous system. *Adv Exp Med*
729 *Biol* 588:145–155.
- 730 Rocher AB, Crimins JL, Amatrudo JM, Kinson MS, Todd-Brown MA,
731 Lewis J, Luebke JI (2010) Structural and functional changes in tau
732 mutant mice neurons are not linked to the presence of NFTs. *Exp*
733 *Neurol* 223:385–393.
- Roy S, Zhang B, Lee VM-Y, Trojanowski JQ (2005) Axonal transport
734 defects: a common theme in neurodegenerative diseases. *Acta*
735 *Neuropathol* 109:5–13.
- Scip A, Arnaboldi A, Colombo I, Veglianesi P, Colombo L, Messa M,
737 Mancini S, Cimini S, Morelli F, Antoniou X, et al. (2013) Soluble
738 A β oligomer-induced synaptopathy: c-Jun N-terminal kinase's
739 role. *J Mol Cell Biol* 5:277–279.
- Scip A, Tozzi A, Abaza A, Cardinetti D, Colombo I, Calabresi P,
741 Salmona M, Welker E, Borsello T (2014) c-Jun N-terminal kinase
742 has a key role in Alzheimer disease synaptic dysfunction in vivo.
743 *Cell Death Dis* 5:e1019.
- Seibenhener ML, Wooten MC (2015) Use of the Open Field Maze to
745 measure locomotor and anxiety-like behavior in mice. *J Vis Exp*:
746 e52434.
- Shemesh OA, Erez H, Ginzburg I, Spira ME (2008) Tau-induced
748 traffic jams reflect organelles accumulation at points of
749 microtubule polar mismatching. *Traffic* 9:458–471.
- Streng J (1974) Exploration and learning behavior in mice selectively
751 bred for high and low levels of activity. *Behav Genet* 4:191–204.
- Thies E, Mandelkow E-M (2007) Missorting of tau in neurons causes
753 degeneration of synapses that can be rescued by the kinase
754 MARK2/Par-1. *J Neurosci* 27:2896–2907.
- Walsh RN, Cummins RA (1976) The Open-Field Test: a critical
756 review. *Psychol Bull* 83:482–504.
- Yancopoulos D, Spillantini MG (2003) Tau protein in familial and
758 sporadic diseases. *Neuromol Med* 4:37–48.
- Yoshiyama Y, Higuchi M, Zhang B, Huang S-M, Iwata N, Saido TC,
760 Maeda J, Sahara T, Trojanowski JQ, Lee VM-Y (2007) Synapse
761 loss and microglial activation precede tangles in a P301S
762 tauopathy mouse model. *Neuron* 53:337–351.

(Received 2 July 2018, Accepted 28 September 2018)
(Available online xxxx)

764
765
766

UNCORRECTED